Raman gain from waveguides inscribed in $KGd(WO_4)_2$ by high repetition rate femtosecond laser

S. M. Eaton,[1,a] C. A. Merchant,[1] R. Iyer,[1] A. J. Zilkie,[1] A. S. Helmy,[1] J. S. Aitchison,[1] P. R. Herman,[1] D. Kraemer,[2] R. J. D. Miller,[2] C. Hnatovsky,[3] and R. S. Taylor[3]
[1]*Department of Electrical and Computer Engineering, Institute for Optical Sciences, University of Toronto, Toronto M5S 3G4, Canada*
[2]*Department of Chemistry and Physics, Institute for Optical Sciences, University of Toronto, Toronto M5S 3H6, Canada*
[3]*Institute for Microstructural Sciences, National Research Council, Ottawa K1A 0R6, Canada*

(Received 14 August 2007; accepted 23 January 2008; published online 26 February 2008)

We report the formation of waveguides in Raman-active $KGd(WO_4)_2$ with a focused, high repetition rate femtosecond laser. Parallel guiding regions, formed to either side of the laser-induced damage track, supported TE and TM modes that coupled efficiently to optical fiber at telecom wavelengths. Micro-Raman spectroscopy of the guiding regions revealed the preservation of the characteristic 768 and 901 cm^{-1} Raman mode intensities. Raman gain with 6% efficiency was demonstrated for the 768 cm^{-1} Raman line by pumping the waveguide with an infrared 80 ps source, the first time Raman gain has been reported in laser formed waveguides. © *2008 American Institute of Physics*. [DOI: 10.1063/1.2884188]

With the increasing trend toward more compact and efficient optical devices, there has been growing interest in the fabrication of waveguides in nonlinear laser host materials.[1,2] The crystal $KGd(WO_4)_2$ (KGW) is popular for optically active components due to its suitability as a rare-earth host material, high third-order nonlinear susceptibility, high thermal conductivity, and strong Raman conversion properties. KGW has prominent Raman modes at 768 and 901 cm^{-1} arising from the tungsten-oxygen sublattice in the crystal which are useful for wavelength conversion in the near infrared spectrum.[3] In addition, KGW has a short Raman dephasing time on the order of 2.0 ps, making it suitable for picosecond pulse Raman generation devices.[4] Raman lasers have been successfully demonstrated in bulk KGW,[5] and the fabrication of waveguides offers potential for enhanced nonlinear device performance through longer interaction lengths with high confinement. Planar waveguides have been fabricated in KGW using ion implantation techniques,[6] and by growing waveguide films on substrates by pulsed-laser deposition (PLD) techniques.[7] However, there are no known reports of forming single mode waveguides in this material at telecom wavelengths.

Femtosecond laser processing has proven to be a rapid and versatile method of writing waveguides inside both amorphous glasses[8] and crystalline materials such as lithium niobate,[9] quartz,[10] Ti:sapphire,[11] and $KY(WO_4)_2$ (KYW).[12] A benefit of femtosecond laser processing is the nonlinear absorption of the high intensity pulses that confines energy dissipation within the small focal volume of the laser. As a result, localized permanent refractive index modification can be inscribed along an arbitrary three-dimensional path by translating the sample with computer-controlled motion stages. The use of high repetition rate (~1 MHz) femtosecond lasers offers further advantages over other systems such as faster writing speeds and more symmetric waveguides due to cumulative heating effects.[13] One challenge in laser writing of waveguides in a Raman-active material such as KGW is the preservation of the desirable nonlinear crystal properties.

In this letter, we report the formation of low-loss waveguides in crystalline KGW with a high repetition-rate femtosecond laser. Waveguide characterization shows symmetrical waveguide modes on either side of the laser-damage track that match closely with the mode profile of single-mode fiber (SMF). Micro-Raman spectroscopy reveals that the crystalline structure of KGW is preserved in these guiding regions, while laser pumping of the waveguide demonstrated Raman gain.

Waveguides were written in bulk KGW crystal slabs (High Q Laboratories, $30\times13\times1$ mm^3, refractive index =2.0), with an amplified Yb-fiber laser (IMRA μJewel D-400-VR), generating 300 fs pulses at 2 MHz repetition rate and 1045 nm wavelength. Waveguides were optimized over a range of laser exposure conditions, with average power and scan speed varied between 50 to 400 mW and 0.2 to 60 mm/s, respectively. The sample was scanned transversely relative to the incident laser using air-bearing motion stages (Aerotech ABL1000). The laser was focused to a depth of 200 μm with a 0.4 numerical aperture (NA) aspheric lens (~2.2 μm spot size diameter, ~10.8 μm depth of focus) and scanned along the N_m axis of the KGW crystal over a 13 mm length, with the writing beam polarization oriented parallel to the scan direction.

Refractive index profiles of the polished end facets were obtained by microreflectivity measurement[14] Spatially resolved micro-Raman spectra (JY Horiba LabRAM) were recorded by scanning a cw 532 nm excitation laser over a 30×30 μm^2 cross section. The insertion loss of the written waveguides was characterized by launching light from a 1250–1650 nm broadband light source (Agilent 83437A) through the device to an optical spectrum analyzer by using butt-coupled SMF with index matching oil at the facets. To capture the near-field mode profiles, light from a 1550 nm wavelength tunable laser (Photonetics Tunics-BT) was fiber coupled at the input, with the output facet imaged to a charge coupled device camera (Spiricon SCOR20-1550). Propagation losses for transverse electric (TE) and transverse mag-

[a]Electronic mail: shane.eaton@utoronto.ca.

 © 2008 American Institute of Physics
Author complimentary copy. Redistribution subject to AIP license or copyright, see http://apl.aip.org/apl/copyright.jsp

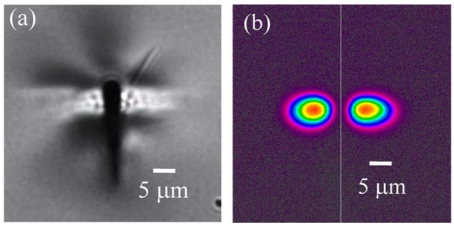

FIG. 1. (Color online) End view (a) of the guiding regions (white regions) and damage track (dark vertical line) recorded with a back-lit microscope and corresponding near-field mode profiles (b) from the adjacent guiding regions at 1550 nm wavelength. The left and right modes were excited individually by translating the input fiber in the transverse direction. The center of the damage track is indicated by the white vertical line. The writing laser was incident from the top.

netic (TM) polarizations were measured with a free-space Fabry-Pérot measurement technique at a wavelength of 1600 nm. TM is defined by electric field polarized vertically (parallel to the incident femtosecond laser) and along the N_p crystal axis, while TE is orthogonal to TM and along the N_g crystal axis. For Raman gain measurements, a 1620 nm wavelength, 80 ps pulse duration laser was coupled into the waveguides with a 40× objective, with output collected by a monochromator (Spectral Products DK240) and liquid nitrogen-cooled detector.

The lowest loss waveguides were found in KGW for exposure conditions of 350 mW average power and 40 mm/s scan speed. An optical microscope cross-sectional view of the femtosecond laser modified zone is shown in Fig. 1(a). The two guiding regions are located laterally on opposite sides of an opaque laser damage track (dark vertical line) of $\sim 4\times 25\ \mu m^2$ dimension that exceeds the $\sim 2\times 11\ \mu m^2$ focal dimensions of the laser. The near-field mode profiles are shown in Fig. 1(b) and reveal strong confinement and single mode guiding with $10\times 8\ \mu m^2$ diameters ($1/e^2$ of intensity), well matched to SMF with 10.5 μm mode field diameter. The waveguide modes could only be excited individually by translation of the input single mode fiber, suggesting that this structure defines two independent waveguides. Despite the close proximity of the guiding regions, evanescent coupling was not observed, which we attribute to the damaged and lossy coupling region.

For the optimum writing condition, microreflectivity measurements of the end facet of the crystal revealed an increase in refractive index of $\Delta n \sim 0.006$ over a $10\times 10\ \mu m^2$ region on either side of the damage track, corresponding closely to the $10\times 8\ \mu m^2$ ($1/e^2$ of intensity) mode profiles shown in Fig. 1(b). With free-space launching, the waveguides supported both TE and TM modes, in contrast to the TM guiding reported in lithium niobate[9,15,16] and quartz.[10] The TM-only guiding in lithium niobate was attributed to the stress-optic responses around an expanded, central amorphized region with an elliptical shape.[9] In our case, the modified zones were less symmetric, with elongated shapes leading to a more complex stress distribution. However, there is insufficient data on stress-optic response in KGW to elucidate the mechanisms for TE and TM guidings. Thomson *et al.* have also noted a transition to guiding both polarizations in lithium niobate when exposing with higher energy femtosecond laser pulses.[17]

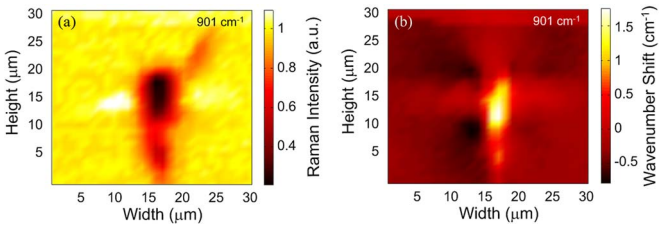

FIG. 2. (Color online) Spatial map of the (a) peak intensity and (b) frequency shift of the 901 cm^{-1} Raman mode with respect to bulk KGW over the two waveguide regions and the central laser-damage region.

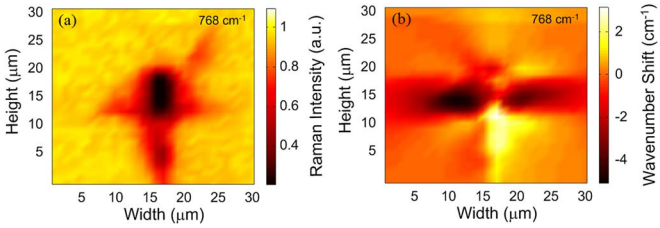

FIG. 3. (Color online) Spatial map of the (a) peak intensity and (b) frequency shift of the 768 cm^{-1} Raman mode with respect to bulk KGW over the two waveguide regions and the central laser-damage region.

Using the Fabry-Pérot technique, propagation losses of 2.0 and 2.6 dB/cm for TE and TM polarizations were measured at 1600 nm wavelength, respectively, for the left mode shown in Fig. 1(b). Losses for the right mode were slightly higher, at 3.4 and 4.0 dB/cm for the TE and TM polarizations, respectively. These propagation losses are comparable with the 3 dB/cm loss reported for KGW waveguide films fabricated by PLD.[7]

For the left mode, insertion losses obtained by launching light with SMF decreased from 4 to 2.2 dB as the wavelength increased from 1250 to 1650 nm. A propagation loss of 1.8 dB/cm at 1600 nm wavelength was inferred from the 2.5 dB insertion loss after accounting for the mode-mismatch coupling loss of 0.2 dB, calculated by the mode overlap integral. This propagation loss is slightly less than 2–2.6 dB/cm values inferred from the Fabry-Pérot technique due to unaccounted losses from imperfect nonorthogonal alignment of waveguides and end facets.[18]

Recently, waveguide formation was reported in Yb-doped KYW crystal,[12] a similar class of host material to KGW, by using a 1 kHz femtosecond laser. A guiding region was formed above the damage track as opposed to the lateral guiding regions found here with the 2 MHz repetition rate laser. To improve transverse confinement in KYW, the authors inscribed two parallel damage tracks separated by 15 μm that exhibited a larger mode of $\sim 20\ \mu$m diameter and a similar propagation loss of ~ 4 dB/cm at 1 μm wavelength in comparison with the present KGW results.[12] Burghoff *et al.* first demonstrated this parallel writing method for improving mode confinement and symmetry in femtosecond-laser written lithium niobate[9,15] waveguides. In KGW, well-confined TE/TM modes were demonstrated with only a single exposure track, yielding faster writing time and more facile waveguide optimization due to one fewer experimental variable.

The Raman response around the laser-formed guiding region was examined for the optimum low-loss waveguide formation condition. The most efficient Raman conversion occurs when the guided light is polarized in the TE direction (N_g axis). The peak intensity of this Raman mode is directly related to the steady-state Raman gain parameter,[4] thereby permitting one to directly infer stimulated Raman scattering

Author complimentary copy. Redistribution subject to AIP license or copyright, see http://apl.aip.org/apl/copyright.jsp

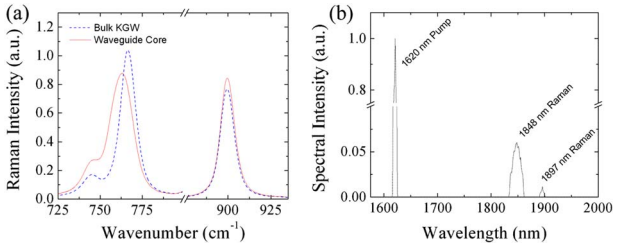

FIG. 4. (Color online) Raman intensity (a) present in waveguide core (solid line) and bulk (dashed line) and spectrum (b) of 1620 nm pump laser and generated Raman lines at 1848 and 1897 nm wavelength, measured by monochromator and cooled detector.

response from measured changes in the Raman spectrum. Wavelength shifts in the Raman mode will correspondingly change the wavelength conversion properties of the device, as well as indicate localized stress regions. Figures 2 and 3 show the intensity maps and spectral shifts of the two prominent Raman modes at 901 and 768 cm^{-1}, respectively. For the 901 cm^{-1} peak, the intensity of the Raman line in Fig. 2(a) is seen to increase by ~10% in the guiding regions of the crystal located on either side of the central damage track. In the center of the damage track, the Raman intensity drops to less than 20% of the value of unmodified KGW, suggesting strong damage to the crystal lattice by the femtosecond laser interaction, which is consistent with studies of femtosecond-laser-induced damage in other crystals.[9–12] The peak location of the 901 cm^{-1} Raman mode in Fig. 2(b) is seen to blueshift slightly by +0.5 cm^{-1} in the guiding regions, and by even higher shifts of +1.7 cm^{-1} in the damage region where there is a reduced peak intensity. Raman shifts have been used previously to characterize stress in $PbWO_4$ which has similar Raman modes as KGW from the tungstate sublattice. Since the positive/negative frequency shifts of the 902 cm^{-1} Raman mode in $PbWO_4$ indicated compressive/tensile stresses, we can infer the formation of compressive stresses in the waveguiding region of KGW where positive Raman shifts [Fig. 2(b)] were observed. However, further crystal analysis is necessary to calibrate the present Raman shifts quantitatively against compressive and tensile stress for KGW.

The intensity map of the 768 cm^{-1} Raman mode in Fig. 3(a) shows an ~20% reduction of the Raman intensity in the waveguiding regions, contrary to the enhancement seen with the 901 cm^{-1} peak in Fig. 2(a). Figure 3(b) shows the 768 cm^{-1} Raman mode to redshift by approximately −5 cm^{-1} in the guiding region to 763 cm^{-1}. In the damage track region, a blueshift of about 2 cm^{-1} was observed along with a strong reduction in Raman intensity, similar to the 901 cm^{-1} peak behavior. This crystal vibrational mode has not previously been characterized for stress response in other tungstate crystals,[19] but the observed negative frequency shift suggests a sensitive indicator for the compressive stresses anticipated in the waveguiding regions. Overall, the micro-Raman intensity and frequency shift observations reveal good preservation of the 768 cm^{-1} Raman mode response, and slight enhancement of the 901 cm^{-1} Raman mode response in the waveguiding regions, thus offering good promise for Raman-active optical devices in KGW crystal.

The Raman spectra are presented in Fig. 4(a), showing small intensity changes and −5.0 and +0.5 cm^{-1} shifts in the waveguide relative to the bulk for the 768 and 901 cm^{-1} Raman modes, respectively. When 80 ps duration pump laser light at 1620 nm wavelength was coupled into the KGW waveguide, Raman gain was observed at 1848 and 1897 nm wavelengths, as shown in Fig. 4(b). The lines correspond to the respective 763 and 901 cm^{-1} Raman modes measured by micro-Raman spectroscopy [Fig. 4(a)]. To the best of our knowledge, the Raman-generated wavelengths in Fig. 4(b) are the first demonstration of Raman gain in laser formed waveguides, and the first time Raman gain has been observed in KGW waveguides. Although low pump laser pulse energy of 200 nJ (~1 GW/cm^2 peak intensity coupled to waveguide) was necessary to avoid facet damage, moderately good conversion efficiencies of 6% and 1% were obtained for 763 and 901 cm^{-1} Raman modes, respectively, as inferred from Fig. 4(b).

In summary, a focused high repetition rate femtosecond laser was used to form damage tracks in crystalline KGW, yielding adjacent zones of compressive stress in which single mode guiding was demonstrated in the telecom spectrum. Micro-Raman spectroscopy showed that Raman responses were preserved in the guiding regions. The waveguide modes showed low polarization dependence, and coupled efficiently to single-mode fiber, which is attractive for integration with standard telecom devices. Raman gain was demonstrated with a conversion efficiency of 6% for the 901 cm^{-1} Raman line with 1620 nm, the first time Raman gain has been shown in laser written waveguides.

[1] M. Shimokozono, N. Sugimoto, A. Tate, Y. Katoh, M. Tanno, S. Fukuda, and T. Ryuoh, Appl. Phys. Lett. **68**, 2177 (1996).
[2] Y. E. Romanyuk, C. N. Borca, M. Pollnau, S. Rivier, V. Petrov, and U. Griebner, Opt. Lett. **31**, 53 (2006).
[3] A. Major, J. S. Aitchison, P. W. E. Smith, N. Langford, and A. I. Ferguson, Opt. Lett. **30**, 421 (2005).
[4] T. T. Basiev, V. V. Osiko, A. M. Prokhorov, and E. M. Dianov, Top. Appl. Phys. **89**, 351 (2003).
[5] K. Andryunas, Y. Vishakas, V. Kabelka, I. V. Mochalov, A. Pavlyuk, G. Petrovskii, and V. Syrus, JETP Lett. **42**, 410 (1986).
[6] C. A. Merchant, J. S. Aitchison, S. Garcia-Blanco, C. Hnatovsky, R. S. Taylor, F. Agullo-Rueda, A. J. Kellock, and J. E. E. Baglin, Appl. Phys. Lett. **89**, 111116 (2006).
[7] P. A. Atanasov, T. Omato, R. I. Tomov, and M. Obara, Thin Solid Films **453-454**, 150 (2004).
[8] K. M. Davis, K. Miura, N. Sugimoto, and K. Hirao, Opt. Lett. **21**, 1729 (1996).
[9] J. Burghoff, S. Nolte, and A. Tünnermann, Appl. Phys. A: Mater. Sci. Process. **89**, 127 (2007).
[10] T. Gorelik, M. Will, S. Nolte, A. Tünnermann, and U. Glatzel, Appl. Phys. A: Mater. Sci. Process. **76**, 309 (2003).
[11] V. Apostolopolous, L. Laversenne, T. Colomb, C. Depeursinge, R. P. Salathe, M. Pollnau, R. Osellame, G. Cerullo, and P. Laporta, Appl. Phys. Lett. **85**, 1122 (2004).
[12] C. N. Borca, V. Apostolopoulos, F. Gardillou, H. G. Limberger, M. Pollnau, and R. P. Salathe, Appl. Surf. Sci. **253**, 8300 (2007).
[13] C. B. Schaffer, A. Brodeur, and E. Mazur, Meas. Sci. Technol. **12**, 1784 (2001).
[14] R. S. Taylor, C. Hnatovsky, E. Simova, D. M. Rayner, M. Mehandale, V. R. Bhardwaj, and P. B. Corkum, Opt. Express **11**, 775 (2003).
[15] J. Thomas, M. Heinrich, J. Burghoff, S. Nolte, A. Ancona, and A. Tünnermann, Appl. Phys. Lett. **91**, 151108 (2007).
[16] H. T. Bookey, R. R. Thomson, N. D. Psaila, A. Kar, N. Chiodo, R. Osellame, and G. Cerullo, IEEE Photonics Technol. Lett. **19**, 892 (2007).
[17] R. R. Thomson, S. Campbell, I. J. Blewett, A. K. Kar, and D. T. Reid, Appl. Phys. Lett. **88**, 111109 (2006).
[18] C. Florea and K. A. Winick, J. Lightwave Technol. **21**, 246 (2003).
[19] W. L. Zhu, K. S. Wan, Y. L. Huang, X. Q. Feng, and G. Pezzotti, Phys. Status Solidi A **203**, 2376 (2006).

Author complimentary copy. Redistribution subject to AIP license or copyright, see http://apl.aip.org/apl/copyright.jsp